Beyond light's limits: Fluorescence imaging at the nanoscale

Fluorescent probes for three super-resolution modalities—STORM, SIM, and STED microscopy.

Recent advances in optics, instrumentation, and software have led to the parallel development of methods designed to increase the resolution of light microscopy beyond that dictated by the wavelength of light. And with these super-resolution microscopy (SRM) techniques comes unprecedented clarity in commonly observed cell biology features, including organelle structure, co-localization, and translocation.

In conventional microscopy, a single fluorophore (less than a few nanometers in diameter) can only be resolved as a point spread function (PSF) that is roughly half the light wavelength for lateral resolution and twice that in depth, due to interactions between visible light and the surrounding media; the PSF is typically estimated as ~250 nm in the x and y directions and ~450–700 nm in the z direction [1]. As a consequence, the images of two or more fluorophores within a few hundred nanometers of one another become blurred together, limiting resolution.

Here we focus on Molecular Probes® fluorescent dyes and labels for three SRM techniques: STORM, SIM, and STED microscopy. These SRM modalities are approaching the resolution historically reserved for electron microscopy, while also providing the inherent benefits of selective targeting and multiplexing for biological context.

STORM: Stochastic optical reconstruction microscopy

The SRM method STORM utilizes stochastic activation and time-resolved localization of photoswitchable fluorophores to generate high-resolution images. Photoswitching dyes must have high photon outputs per switch, coupled with a low duty cycle (i.e., they are in a non-emitting state longer than in an emitting state). With appropriate dye–buffer combinations, an optimized STORM system can generate images with 5 nm resolution. Two forms of STORM exist. The first approach utilizes two dyes: an "activator" to induce switching and a "reporter" from which emission is detected [2]. The second approach, commonly known as direct STORM or dSTORM, relies upon direct switching of the fluorophore through specific excitation parameters [3].

The activator–reporter STORM method requires dual labeling of an affinity reagent, such as an antibody, with a reactive dye [4]. Many Alexa Fluor® dyes, including Alexa Fluor® 405 dye [5–8], Alexa Fluor® 488 dye [8], and Alexa Fluor® 555 dye [8], have been used as effective activators; both Alexa Fluor® 647 dye [4,6–11] and Alexa Fluor® 750 dye [9] have been shown to be reliable reporters. For example, STORM imaging has been used to visualize mitochondria and microtubules using Alexa Fluor® 405 and Cy®3 dyes as activators together with Alexa Fluor® 647 dye as the reporter (Figure 1). The availability of multiple activator–reporter pairs facilitates multicolor STORM that uses as many as six fluorescence channels simultaneously [8].

Surprisingly, quite efficient photoswitching can be induced without an activator dye [3]. With the dSTORM method, many Alexa Fluor® dyes have been shown to be able to photoswitch in this manner [12–15], including:

- Alexa Fluor® 488
- Alexa Fluor® 532
- Alexa Fluor® 568
- Alexa Fluor® 647
- Alexa Fluor® 680
- Alexa Fluor® 700
- Alexa Fluor® 750
- Alexa Fluor® 790

In particular, Alexa Fluor® 647 dye is used extensively in dSTORM because it has proven to exhibit extremely good photoswitching properties [15], namely, high photon output, cycle number, and survival fraction, along with a low duty cycle. Figure 2 shows comparative wide-field and dSTORM imaging of keratin using an Alexa Fluor® 647 dye–labeled secondary antibody; →

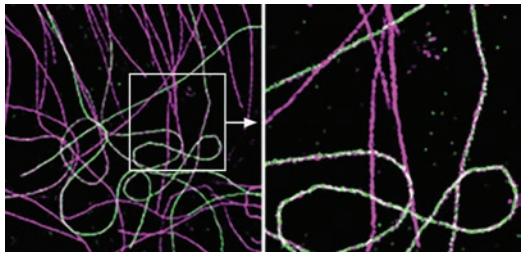

Figure 1. Two-color STORM imaging of microtubules. BS-C-1 cells were aldehyde-fixed, reduced with sodium borohydride, and labeled with primary antibodies to tyrosinated or detyrosinated tubulin. Tyrosinated tubulin was stained with an Alexa Fluor® 647 secondary antibody (pseudocolored magenta), and detyrosinated tubulin was stained with an Alexa Fluor® 750 secondary antibody (pseudocolored green). Image (left) and zoom-in image (right) from the boxed region provided by Joshua Vaughan, Graham Dempsey, Eileen Sun, and Xiaowei Zhuang, Harvard University.

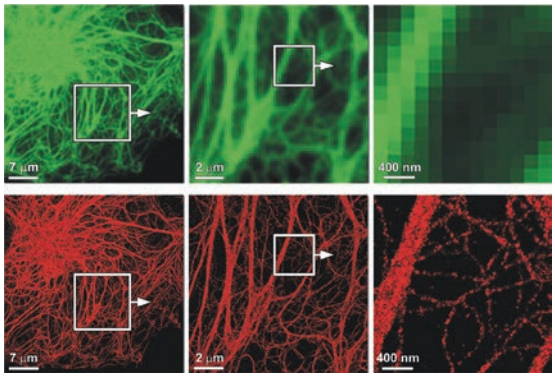

Figure 2. Single-color dSTORM imaging of keratin using an Alexa Fluor® 647 secondary antibody conjugate. PtK cells were fixed and labeled with an anti-keratin antibody, followed by a species-specific Alexa Fluor® 647 secondary antibody conjugate. Total internal reflection fluorescence (TIRF, top row) and dSTORM (bottom row) images and zoom-in images from the boxed regions provided by Michael W. Davidson, Florida State University. The TIRF images were color-shifted to increase overall contrast.

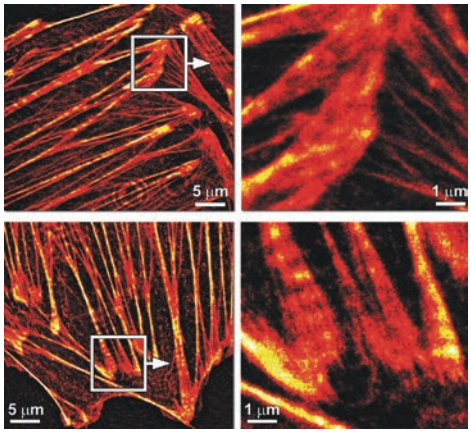

Figure 3. Single-color dSTORM imaging of the actin cytoskeleton using Alexa Fluor® phalloidin conjugates. The actin cytoskeleton was labeled using Alexa Fluor® 488 phalloidin (top, Cat. No. A12379) or Alexa Fluor® 568 phalloidin (bottom, Cat. No. A12380). Images (left column) and zoom-in images (right column) from the boxed regions provided by John Allen, Florida State University.

note the greatly improved resolution in the dSTORM image. Implementation of multicolor dSTORM is critically dependent on the imaging buffer systems that facilitate switching events. Several recent studies have characterized the buffer systems required to perform multicolor imaging using Alexa Fluor® dyes; see **lifetechnologies.com/srmbp70** for details.

STORM imaging is not limited to the detection of cellular targets with antibodies. Many other Alexa Fluor® conjugates have been used, including those of cholera toxin B [16], phalloidin [17–19] (Figure 3), dextran [17,18], EGF [17,18], transferrin [7], and WGA [20,21]; DNA synthesis has been detected using Click-iT® EdU Alexa Fluor® assays [12,22]. Moreover, STORM has been demonstrated in live cells using Alexa Fluor® dyes [7], as well as MitoTracker® Red, LysoTracker® Red, ER-Tracker™ Red, and DiI organelle-selective probes [23], and the nucleic acid stains SYTO® 13 and YOYO®-1 [12].

SIM: Structured illumination microscopy

In SIM, structured illumination is employed to enhance spatial resolution. The sample is first illuminated with patterned light, and then the information in the Moire fringes that lie outside of the normal range of observation is analyzed [24]. Reconstruction software deciphers the images to give a resolution limit of about 100 nm (two-fold higher resolution than the diffraction limit of 250 nm).

SIM is the best choice for super-resolution microscopy when imaging live cells or thick tissue sections or for 3D imaging because it combines imaging speed with improved resolution. SIM places higher pressure on the photostability of the label; therefore, choosing the brightest and most photostable fluorophores and using an effective antifade (see a description of ProLong® Diamond Antifade Mountant in the "Just Released" section on page 3) will significantly enhance SIM data. Alexa Fluor® 488 dye [25–35], Alexa Fluor® 555 dye [27,31,33,36], Alexa Fluor® 568 dye [28,32], and Alexa Fluor® 594 dye [25,26,29,30,34,35] are all commonly used in combination with one another, and they represent the most intensely fluorescent and photostable probes for the filter sets commonly found on commercial SIM systems. SIM imaging has also been demonstrated using fluorescent proteins [37–39]. Figure 4 shows SIM imaging using two Molecular Probes® ready-to-use targeted fluorescent protein constructs, CellLight® Mitochondria-GFP and CellLight® Golgi-RFP.

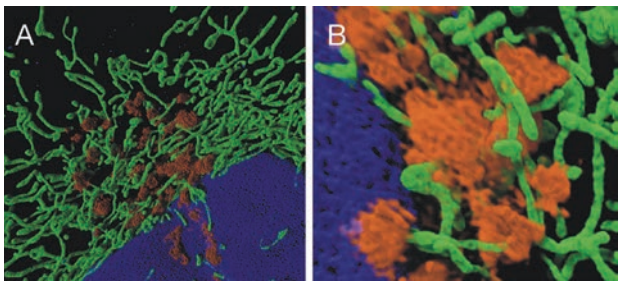

Figure 4. Three-color SIM imaging using fluorescent proteins. HeLa cells were transduced with CellLight® Mitochondria-GFP (Cat. No. C10508) and CellLight® Golgi-RFP (Cat. No. C10593), stained with Hoechst® 33342 dye (Cat. No. H1399), and imaged using the DeltaVision OMX SIM system. Image **(A)** and zoom-in image **(B)** from a slightly different field of view provided by Ian Clements, GE Healthcare.

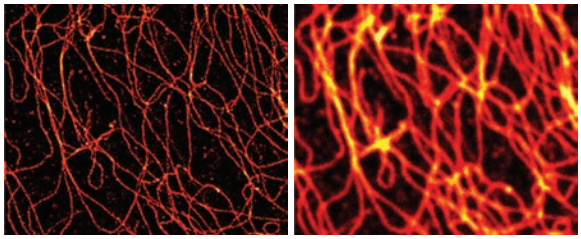

Figure 5. STED microscopy of intermediate filaments visualized with Oregon Green® 488 staining. PtK2 cells were methanol-fixed, and vimentin was labeled with Oregon Green® 488 dye by indirect immunofluorescence. Confocal **(A)** and STED **(B)** images were acquired with a Leica TCS STED CW microscope. Images provided by Leica Microsystems.

STED microscopy: Stimulated emission depletion microscopy

The first technique to break the diffraction limit, STED microscopy uses two laser pulses to localize fluorescence at each focal spot. The first pulse is used to excite a fluorophore to its fluorescent state, and the second pulse is a modified beam used to de-excite (through stimulated emission depletion) any fluorophores surrounding the excitation focal spot [40]. The focal spot is raster scanned across the sample to generate an image, and the acquisition speed is relatively slow for large fields of view. One advantage of STED microscopy is the large depth of view (10–15 µm) that can be imaged with high resolution (30 nm in x and y resolution, with z resolution comparable to that of conventional confocal microscopy).

When choosing dyes for STED, one must be careful to select exceptionally stable fluorophores whose properties match the depletion laser lines available. Alexa Fluor® 488 dye [41–43], Alexa Fluor® 594 dye [44,45], and Oregon Green® 488 dye [43] have each been used for STED, either on their own (Figure 5) or together for multicolor STED [35]. Alexa Fluor® 488 dye has also been used in combination with Pacific Orange™ dye for dual-color STED [46,47].

The future of fluorescence microscopy

Although super-resolution technologies do not yet meet the resolution achieved by electron microscopy, advances in cameras, optics, algorithms, and fluorescent probes are expected to continue to improve both the resolution and multicolor capabilities. Widely cited in SRM applications, Molecular Probes® fluorophores and targeted fluorescent conjugates are at the forefront of these developments. Use our online SRM selection guides to find products as well as recent references for STORM, SIM, and STED microscopy at **lifetechnologies.com/srmbp70**. ■

Table 1. Published articles citing Molecular Probes® fluorescent dyes for super-resolution microscopy.

STORM including dSTORM

1. Galbraith CG, Galbraith JA (2011) *J Cell Sci* 124:1607–1611. **2.** Rust MJ, Bates M, Zhuang X (2006) *Nat Methods* 3:793–795. **3.** Heilemann M, van de Linde S, Schüttpelz M et al. (2008) *Angew Chem Int Ed Engl* 47:6172–6176. **4.** Bates M, Jones SA, Zhuang X (2013) *Cold Spring Harb Protoc* 2013:540–541. **5.** Xu K, Zhong G, Zhuang X (2013) *Science* 339:452–456. **6.** Dani A, HuWang B, Bergan J et al. (2010) *Neuron* 68:843–856. **7.** Jones SA, Shim SH, He J et al. (2011) *Nat Methods* 8:499–508. **8.** Huang B, Jones SA, Brandenburg B et al. (2008) *Nat Methods* 5:1047–1052. **9.** Bates M, Dempsey GT, Chen KH (2012) *Chemphyschem* 13:99–107. **10.** Lakadamyali M, Babcock H, Bates M et al. (2012) *PLoS One* 7:e30826. **11.** Mukamel EA, Babcock H, Zhuang X (2012) *Biophys J* 102:2391–2400. **12.** Allen JR, Ross ST, Davidson MW (2013) *J Opt* 15:094001. **13.** van de Linde S, Aufmkolk S, Franke C et al. (2013) *Chem Biol* 20:8–18. **14.** Baddeley D, Crossman D, Rossberger S (2011) *PLoS One* 6:e20645. **15.** Dempsey GT, Vaughan JC, Chen KH (2011) *Nat Methods* 8:1027–1036. **16.** Vaughan JC, Dempsey GT, Sun E et al. (2013) *J Am Chem Soc* 135:1197–1200. **17.** Metcalf DJ, Edwards R, Kumarswami N et al. (2013) *J Vis Exp* 79:50579. **18.** Rees EJ, Erdelyi M, Pinotsi D et al. (2012) *Optical Nanoscopy* 1:12. **19.** Rossi A, Moritz TJ, Ratelade J et al. (2012) *J Cell Sci* 125:4405–4412. **20.** Babcock H, Sigal YM, Zhuang X (2012) *Optical Nanoscopy* 1:6. **21.** Löschberger A, van de Linde S, Dabauvalle MC et al. (2012) *J Cell Sci* 125:570–575. **22.** Zessin PJ, Finan K, Heilemann M (2012) *J Struct Biol* 177:344–348. **23.** Shim SH, Xia C, Zhong G et al. (2012) *Proc Natl Acad Sci U S A* 109:13978–13983.

SIM

24. Gustafsson MG (2000) *J Microsc* 198:82–87. **25.** Al-Hakim AK, Bashkurov M, Gingras AC (2012) *Mol Cell Proteomics* 11:*M*111.014233. **26.** Green LC, Kalitsis P, Chang TM et al. (2012) *J Cell Sci* 125:1591–1604. **27.** Mennella V, Keszthelyi B, McDonald KL et al. (2012) *Nat Cell Biol* 14:1159–1168. **28.** Munck S, Miskiewicz K, Sannerud R et al. (2012) *J Cell Sci* 125:2257–2266. **29.** Sonnen KF, Schermelleh L, Leonhardt H et al. (2012) *Biol Open* 1:965–976. **30.** Guizetti J, Schermelleh L, Mäntler J et al. (2011) *Science* 331:1616–1620. **31.** Baddeley D, Chagin VO, Schermelleh L et al. (2010) *Nucleic Acids Res* 38:e8. **32.** Duleh SN, Welch MD (2010) *Cytoskeleton* (Hoboken) 67:193–206. **33.** Nakamura AJ, Rao VA, Pommier Y et al. (2010) *Cell Cycle* 9:389–397. **34.** Mancuso G, Gambuzza M, Midiri A et al. (2009) *Nat Immunol* 10:587–594. **35.** Britton S, Coates J, Jackson SP (2013) *J Cell Biol* 202:579–595. **36.** Zlatic SA, Grossniklaus EJ, Ryder PV et al. (2013) *Mol Biol Cell* 24:2378–2388. **37.** York AG, Parekh SH, Dalle Nogare D et al. (2012) *Nat Methods* 9:749–754. **38.** Fitzgibbon J, Bell K, King E (2010) *Plant Physiol* 153:1453–1463. **39.** Kner P, Chhun BB, Griffis ER et al. (2009) *Nat Methods* 6:339–342.

STED microscopy

40. Klar TA, Jakobs S, Dyba M et al. (2000) *Proc Natl Acad Sci U S A* 97: 8206–8210. **41.** Tønnesen J, Nadrigny F, Willig KI et al. (2011) *Biophys J* 101:2545–2552. **42.** van den Bogaart G, Meyenberg K, Risselada HJ et al. (2011) *Nature* 479:552–555. **43.** Vicidomini G, Moneron G, Han KY et al. (2011) *Nat Methods* 8:571–573. **44.** Takasaki KT, Ding JB, Sabatini BL (2013) *Biophys J* 104:770–777. **45.** Mellroth P, Daniels R, Eberhardt A et al. (2012) *J Biol Chem* 287:11018–11029. **46.** Foster DB, Ho AS, Rucker J et al. (2012) *Circ Res* 111:446–454. **47.** Mace EM, Orange JS (2012) *Commun Integr Biol* 5:184–186.